Supporting Information

pH-Induced Mechanistic Changeover From Hydroxyl Radicals to Iron(IV) in the Fenton Reaction

Hajem Bataineh, Oleg Pestovsky* and Andreja Bakac*

Ames Laboratory and the Department of Chemistry, Iowa State University, Ames, IA 50011

Contents

Additional experimental detail

The following chemicals were obtained commercially and used as received: iron(II) perchlorate hydrate (98%), iron(III) perchlorate hydrate (low chloride < 0.005%), deuterio perchloric acid $DClO_4$ (68 wt% in D_2O, 99+ atom % D), titanium(IV) oxysulfate (99.99% purity, 15 wt% solution in dilute sulfuric acid), deuterium oxide (99.9 atom %D), (R)-(+)-methyl *p*-tolyl sulfoxide (99%), and 1,10-phenanthroline (99+ %) (all Aldrich), dimethyl sulfoxide (≥ 99.9%, A.C.S spectrophotometric grade, Sigma-Aldrich), sodium hydroxide (99.1%), hydrogen peroxide (30 wt%), perchloric acid (70 wt%), anhydrous dibasic sodium phosphate (all Fisher), monobasic

sodium phosphate monohydrate (Baker) piperazine-N,N'-bis(4-butanesulfonic acid) (PIPBS), 4-(N-morpholino)butanesulfonic acid (MOBS), 3-(N-morpholino)-propanesulfonic acid (MOPS), and 2-(N-morpholino)ethanesulfonic acid (MES) (all GFS).

Stock solutions of iron(II) perchlorate in H_2O or D_2O were prepared freshly before each set of experiments and standardized with phenanthroline. Solutions of H_2O_2 were standardized with titanium oxysulfate[1] which places a reliable detection limit at 0.02 mM H_2O_2. Deionized water was further purified by passage through a Barnstead Easy Pure II -UV/UF water purifier.

UV-Vis absorbance measurements and kinetic studies used a Shimadzu UV-3101 PC spectrophotometer, Olis RSM-1000 stopped-flow instrument, and Applied Photophysics (APP) sequential stopped-flow DX-17MV at 25.0 ± 0.1 °C. Gaseous products were analyzed by an Agilent Technologies 7890A GC gas chromatograph equipped with a FID detector and a 15-m capillary column (GS-GASPRO), 0.320 mm I.D. Nitrogen flow rate was constant at 25 cm^3/s. Both the split injector (1:40) and FID detector were held at 200^0 C. The initial oven temperature was 40^0 C, and was increased by 10^0 C/min. ^{1}H-NMR spectra were recorded with a 400 MHz Bruker DRX-400 spectrometer at room temperature. The pH was measured with an Accumet AP71 pH meter. Kinetic experiments were performed at 25.1 ±0.1^0 C.

Procedures All of the solutions were purged with argon before mixing and appeared clear to the eye in both tertiary amine and phosphate buffers prior to and during the reaction. The solvent was H_2O for kinetic studies, and D_2O for NMR product analysis. The pH (pD) was controlled with noncoordinating tertiary amine buffers MES (pK_a 6.06), MOPS (pK_a 7.09), MOBS (pK_a 7.48) and PIPBS (pK_{a1} 4.29, pK_{a2} 8.55)[2] or with phosphate buffers (pH 6-8). Buffer concentrations were typically 8-50 times greater than the concentration of the limiting reagents, i. e. at the level required to hold the pH at the desired value without interfering with the NMR

spectra or altering the chemistry. The pH decrease in kinetics experiments was less than 0.2 units. In the NMR experiments, which typically used 1-2 mM of Fe(II) and H_2O_2, the pD decrease was typically 0.3-0.5 units. Solutions were acidified before the NMR spectra were recorded. Concentrations of Fe(II) in spent reaction solutions were determined with phenanthroline. A correction was applied for the absorbance of iron(III)-phenanthroline as previously described.[3]

The stoichiometry was determined from absorbance changes at 270 nm using $\Delta\varepsilon_{270}$ = 2650±50 M^{-1} cm^{-1} at pH 6-7. This value was determined by oxidizing a solution of Fe(II) (0.010 - 0.020 mM) with excess H_2O_2 (0.1 - 1.5 mM) in the stopped-flow and monitoring the absorbance for up to 30 seconds after the completion of the reaction. During this time, the reading remained constant and yielded ε_{270} = 2600±50 M^{-1} cm^{-1}. Several experiments were also performed on a longer time scale by mixing the reagents (0.02 mM Fe(II) and 0.2 mM H_2O_2 in 0.6 mM MES or MOPS buffer) in a spectrophotometric cell and monitoring the absorbance with a conventional spectrophotometer. The absorbance after the completion of the reaction remained constant for at least five minutes and yielded ε_{270} = 2700±50 M^{-1} cm^{-1}. The constancy of ε_{270} on millisecond-to-minute time scale confirms that the turbidity or precipitation of iron(III) did not affect absorbance readings. This point is also illustrated in the kinetic plots in Figures S6-S8. The three experiments had identical initial concentrations of Fe(II) and H_2O_2 (in excess), while the concentration of $(CH_3)_2SO$ was varied. The reaction times varied over a factor of 14, but the overall absorbance change was the same within the experimental error, showing again that changes in the degree of hydrolysis or agglomeration of the Fe(III) product either did not take place or had no effect on the absorbance around 270 nm.

Product analysis by NMR. A solution of hydrogen peroxide was added to a magnetically stirred solution of $Fe(H_2O)_6^{2+}/Fe(H_2O)_5OH^+$ (pK_a = 9.5)[4] and substrate in D_2O buffered at the desired pD under argon. The pH was measured before and after the reaction, and converted to pD by adding 0.4 to the measured value. Immediately after the completion of the reaction, the solutions were acidified to pD 1 with perchloric acid to avoid agglomeration and precipitation of iron(III) hydroxide(s), and the NMR spectrum was run within minutes. Such solutions contained small amounts of unreacted Fe(II) or H_2O_2, but not both, so that no additional oxidation of the substrate could take place after the acidification. Acetonitrile (0.79 mM) was used as internal standard to quantify the products. No shift or broadening of the product resonances was observed in acidified solutions.

In phosphate buffer at pH 7, the products are ethane (60% yield by GC) and methylsulfinate (25% by NMR), indicative of $HO^{\bullet}$ radicals. The resonances were somewhat broadened, most likely because solutions of iron(III) became slightly inhomogeneous during the time required to record the spectrum. The reasons for the lower yields of methylsulfinate are not fully understood, but a portion of the anion may be complexed to the Fe(III) product and thus not detectable by NMR. In acidic solutions, where the binding would be much weaker (pK_a for $CH_3S(O)OH$ is 2.35), the methyl signal for methylsulfinic acid is shifted to 2.50 ppm and appears on the side of the strong $(CH_3)_2SO$ signal (2.55 ppm) which makes the integration imprecise. Under these conditions, a signal for sulfonic acid (2.63 ppm) was also detected, but it was not well separated from DMSO. Control experiments with samples of genuine sulfinic acid confirmed that significant oxidation to sulfonic acid takes place in the time required for (aerobic) manipulation of the solutions and the recording of the spectrum. Despite the difficulties in detecting all of the expected sulfinic acid, the majority of the reaction in phosphate buffers

appears to involve hydroxyl radicals based on the data and arguments in the main text, and on the finding that the yields of the accompanying product, ethane, were much higher, about 60% (Table 1).

$$HO^{\bullet} + (CH_3)_2SO \rightarrow CH_3SO_2H + CH_3^{\bullet} (\rightarrow 0.5\ C_2H_6)$$

Stopped-flow experiments. Aqueous solutions of iron(II) were mixed with the buffer and dmso immediately before the experiment and loaded into one of the stopped-flow syringes. The other syringe was filled with the H_2O_2 solution. The formation of Fe(III) was monitored either at 270 nm with the Applied Photophysics APP DX-17MV instrument or in the 260-320 nm range with an Olis RSM-1000 rapid scan instrument.

List of Figures

Figure S1. ^{1}H NMR spectrum of the products of the reaction of 1.2 mM $Fe(ClO_4)_2$, 1.1 mM H_2O_2 and 36 mM DMSO in MOPS buffer (11 mM). Initial pD 7.6, final pD 7.2. Spectrum was recorded after acidifying reaction mixture to 0.1 M $DClO_4$. The reaction generated (50 ± 5 μM) $DMSO_2$. ^{13}C satellite peaks are denoted with an asterisk.

Figure S2. a) 1H NMR spectrum showing $TMSO_2$ (0.65 ± 0.05 mM) generated in the reaction of 1.8 mM $Fe(ClO_4)_2$, 2.4 mM H_2O_2 and 29 mM TMSO in PIPBS buffer (15 mM). Initial pD 7.1, final pD 5.7. **b)** Control experiment: ^{1}H NMR spectrum of a mixture of H_2O_2 (2.0 mM), TMSO (43 mM) and PIPBS buffer (22 mM) in D_2O, pD 7.1. The spectra were recorded without acidifying the reaction mixtures. ^{13}C satellite peaks are denoted with an asterisk.

Figure S3. ^{1}H NMR spectrum after the completion of the reaction of 1.0 mM $Fe(ClO_4)_2$, 1.0 mM H_2O_2 and 50 mM TMSO in D_2O, phosphate buffer (20 mM). Initial pD 6.6, final pD 6.0. Spectrum was recorded after acidifying reaction mixture to 0.1 M $DClO_4$. ^{13}C satellite peaks are denoted with an asterisk.

Figure S4. 1H NMR spectrum showing $(CH_3)_2SO_2$ (0.26 mM) generated from the reaction of $Fe(ClO_4)_2$ (0.49 mM), H_2O_2 (0.49 mM) and $(CH_3)_2SO$ (190 mM) in D_2O, MES buffer (9.6 mM),

pD 6.7. Spectrum was recorded after acidifying the reaction mixture to 0.1 M $DClO_4$. ^{13}C satellite peaks are denoted with an asterisk.

Figure S5 ^1H NMR spectrum showing $(CH_3)_2SO_2$ (0.49 mM) generated from the reaction of $Fe(ClO_4)_2$ (0.49 mM), H_2O_2 (0.49 mM) and $(CH_3)_2SO$ (950 mM) in MES buffer (9.6 mM), pD 6.70. Spectrum was recorded after acidifying the reaction mixture to 0.1 M $DClO_4$. ^{13}C satellite peaks are denoted with an asterisk.

Figure S6. Kinetic (stopped flow) trace for a reaction between 0.020 mM Fe(II) and 0.78 mM H_2O_2 in the absence of $(CH_3)_2SO$, pH 6.2 (0.56 mM MES)

Figure S7. Kinetic (stopped flow) trace for a reaction between 0.020 mM Fe(II) and 0.78 mM H_2O_2 at 0.50 M $(CH_3)_2SO$, pH 6.2 (0.56 mM MES)

Figure S8. Kinetic (conventional spectrophotometer) trace for a reaction between 0.020 mM Fe(II) and 0.78 mM H_2O_2 at 0.98 M DMSO, pH 6.2 (0.6 mM MES)

Figure S9. Plot of k_{obs} vs $[H_2O_2]$ for the Fe(II)/ H_2O_2 reaction at pH 6.1 (MES buffer). Conditions: $[Fe(ClO_4)_2]_0$ = 0.005 – 0.035 mM, [MES] = 0.25 – 0.55 mM, 25 °C. pH decreased during the reaction by 0.2 units, see text.

Figure S10. Plot of k_{obs} vs $[H_2O_2]$ for the Fe(II)/ H_2O_2 reaction at pH 7 in a MOPS buffer. Conditions: $[Fe(ClO_4)_2]_0$ = 0.008 – 0.015 mM, [MOPS] = 0.5 - 0.6 mM, 25 °C. pH decreased during the reaction by 0.2 units, see text.

Figure S11. Plot of k_{obs} vs [Fe(II)] for the Fe(II)/ H_2O_2 reaction at pH 6.1 in a MES buffer. Conditions: $[H_2O_2]_0$ = 0.005 - 0.02 mM, [MES] = 0.5-0.6 mM, 25 °C. pH decreased during the reaction by 0.2 units, see text.

Figure S12. Representative kinetic trace in phosphate buffer. Conditions: 0.031 mM Fe(II), 1.0 mM H_2O_2, pH 6.1 (0.6 mM phosphate buffer)

Figure S13. Plot of pseudo-first-order rate constants for the reaction of $Fe(ClO_4)_2$ with H_2O_2 against the concentration of H_2O_2 in phosphate buffer. Conditions: $[Fe(ClO_4)_2]$ = 0.018 – 0.030 mM, [phosphate] = 0.60 mM, pH = 6.2.

Figure S14. (a) ^1H NMR spectrum of the reaction mixture after the completion of the reaction between $Fe(ClO_4)_2$ (1.0 mM), H_2O_2 (1.0 mM), and $(CH_3)_2SO$ (5 mM) at pD 1 in the presence of 5 mM MES. The reaction generated CH_3SO_2H and C_2H_6 in amounts comparable to those

obtained in the absence of MES. b) Mixture of MES (5 mM) and H_2O_2 (1 mM), pD 1. c) MES (5 mM), pD 1.

Figures S1-S11

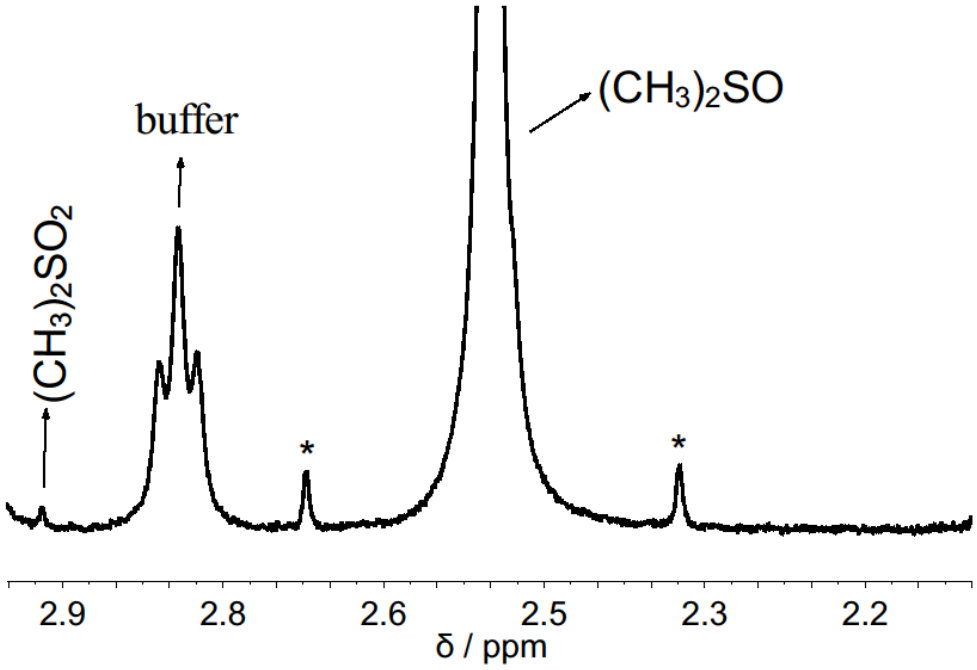

Figure S1. ^{1}H NMR spectrum of the products of the reaction of 1.2 mM $Fe(ClO_4)_2$, 1.1 mM H_2O_2 and 36 mM DMSO in MOPS buffer (11 mM). Initial pD 7.6, final pD 7.2. Spectrum was

recorded after acidifying reaction mixture to 0.1 M $DClO_4$. The reaction generated (50 ± 5 μM) $DMSO_2$. ^{13}C satellites are denoted with an asterisk.

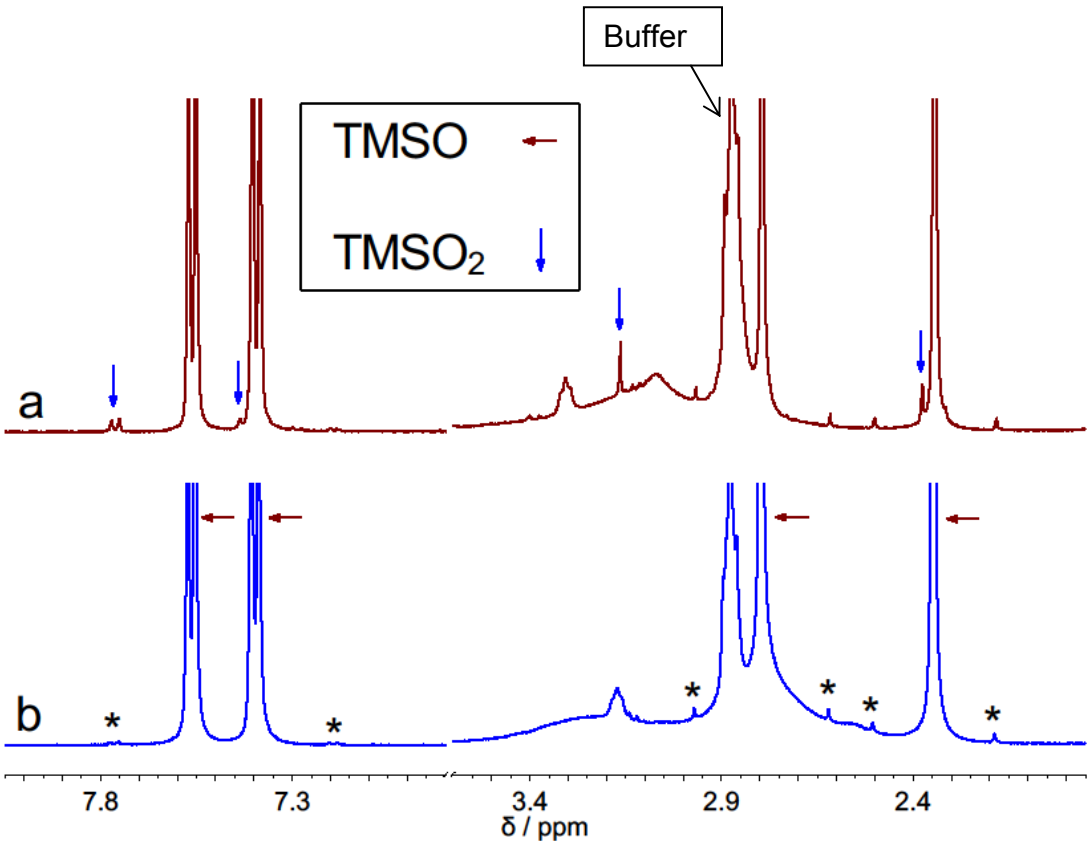

Figure S2. a) 1H NMR spectrum showing $TMSO_2$ (0.65 ± 0.05 mM) generated in the reaction of 1.8 mM $Fe(ClO_4)_2$, 2.4 mM H_2O_2 and 29 mM TMSO in PIPBS buffer (15 mM). Initial pD 7.1, final pD 5.7. **b)** Control experiment: ^1H NMR spectrum of a mixture of H_2O_2 (2.0 mM), TMSO (43 mM) and PIPBS buffer (22 mM) in D_2O, pD 7.1. The spectra were recorded without acidifying the reaction mixtures. ^{13}C satellite peaks are denoted with an asterisk.

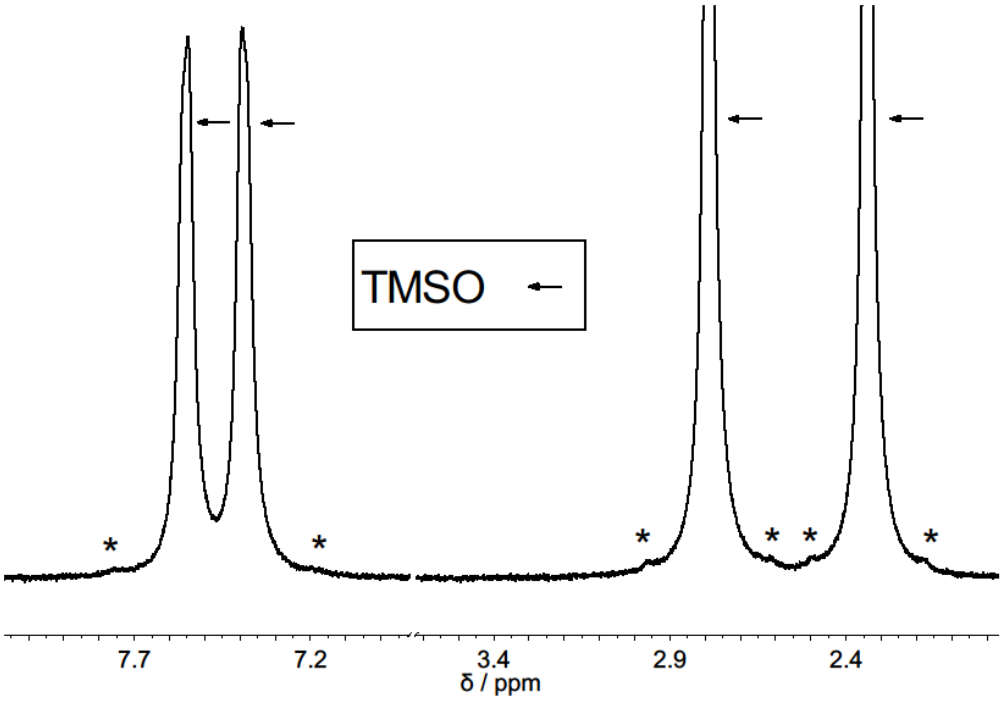

Figure S3. ^{1}H NMR spectrum after the completion of the reaction between 1.0 mM $Fe(ClO_4)_2$, 1.0 mM H_2O_2 and 50 mM TMSO in D_2O, phosphate buffer (20 mM). Initial pD 6.6, final pD 6.0. ^{13}C satellites are denoted with an asterisk.

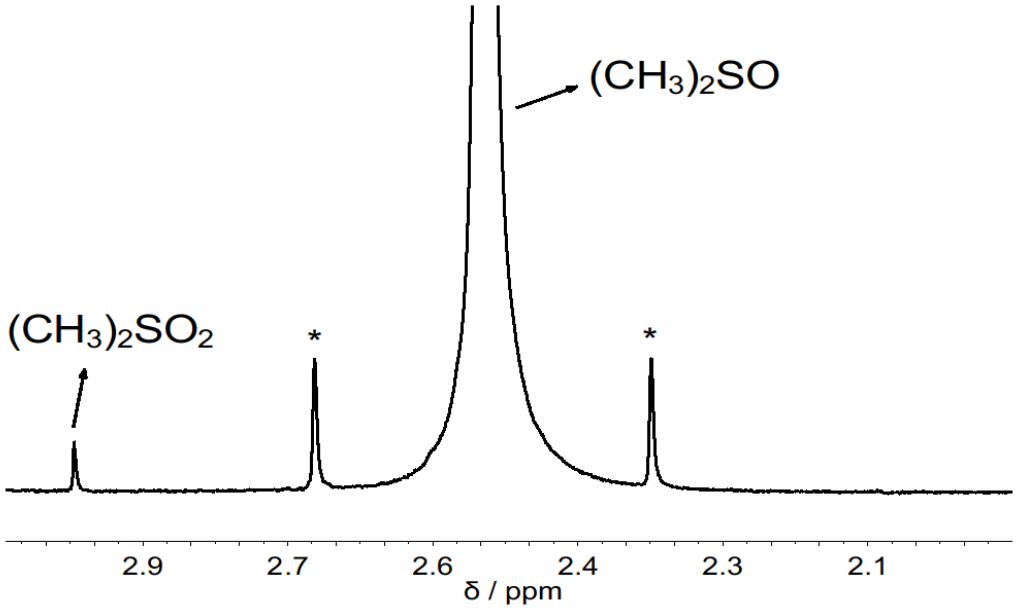

Figure S4. ^{1}H NMR spectrum showing $(CH_3)_2SO_2$ (0.26 mM) generated from the reaction of $Fe(ClO_4)_2$ (0.49 mM), H_2O_2 (0.49 mM) and $(CH_3)_2SO$ (190 mM) in D_2O, MES buffer (9.6 mM), pD 6.7. Spectrum was recorded after acidifying the reaction mixture to 0.1 M $DClO_4$. ^{13}C satellites are denoted with an asterisk.

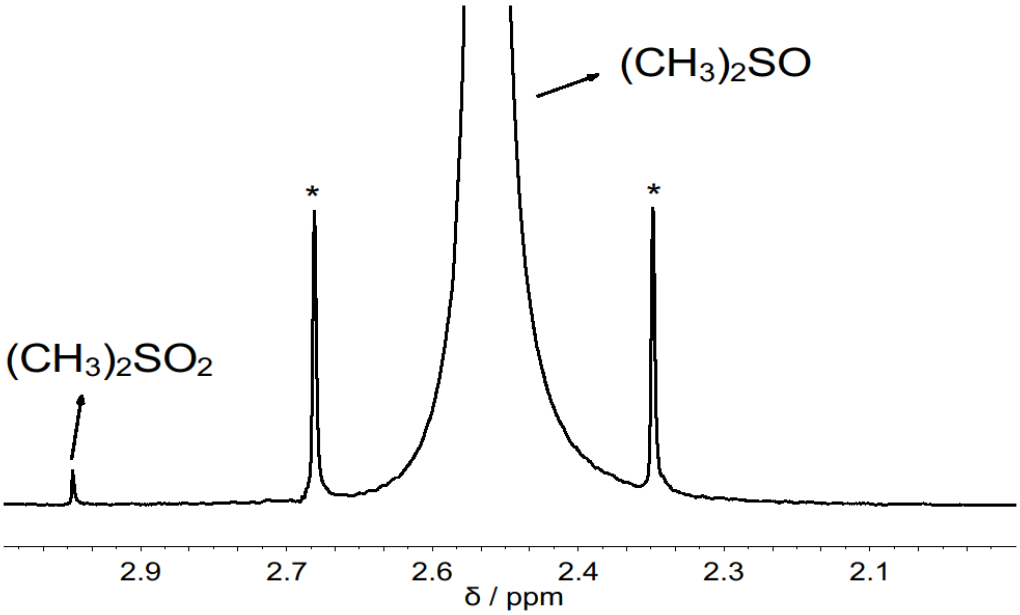

Figure S5 ^{1}H NMR spectrum showing $(CH_3)_2SO_2$ (0.49 mM) generated from the reaction of $Fe(ClO_4)_2$ (0.49 mM), H_2O_2 (0.49 mM) and $(CH_3)_2SO$ (950 mM) in MES buffer (9.6 mM), pD 6.70. Spectrum was recorded after acidifying the reaction mixture to 0.1 M $DClO_4$. ^{13}C satellite peaks are denoted with an asterisk.

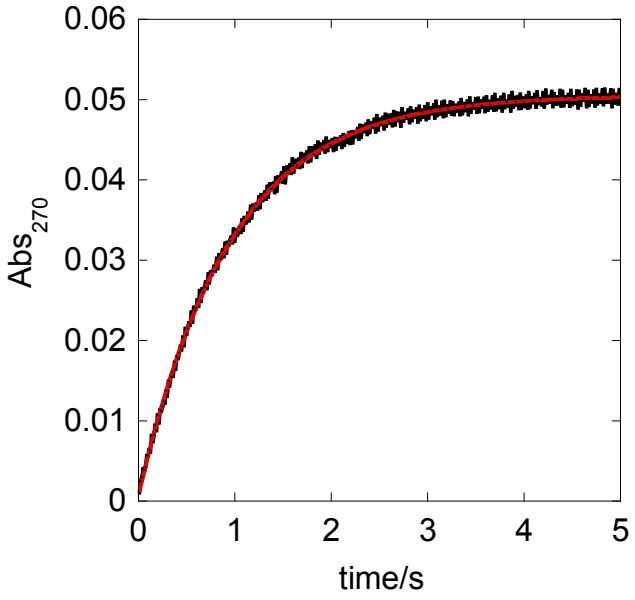

Figure S6. Kinetic (stopped flow) trace for a reaction between 0.020 mM Fe(II) and 0.78 mM H_2O_2 in the absence of DMSO, pH 6.2 (0.56 mM MES)

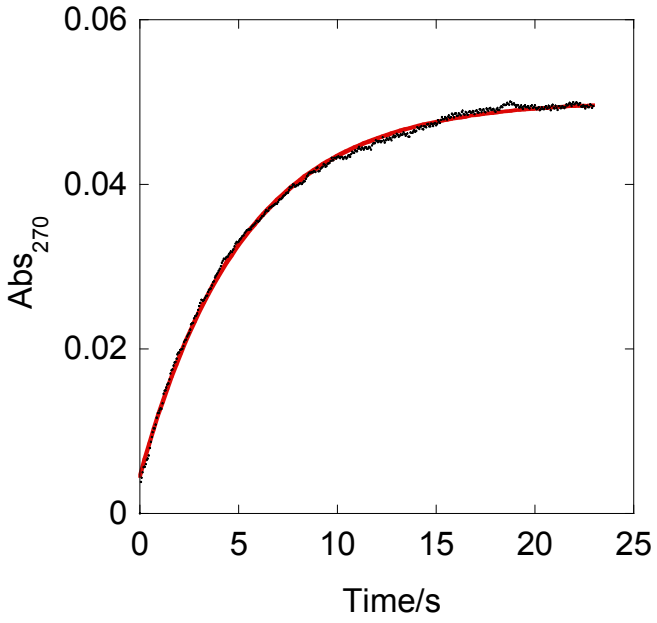

Figure S7. Kinetic (stopped flow) trace for a reaction between 0.020 mM Fe(II) and 0.78 mM H_2O_2 at 0.50 M DMSO, pH 6.2 (0.56 mM MES)

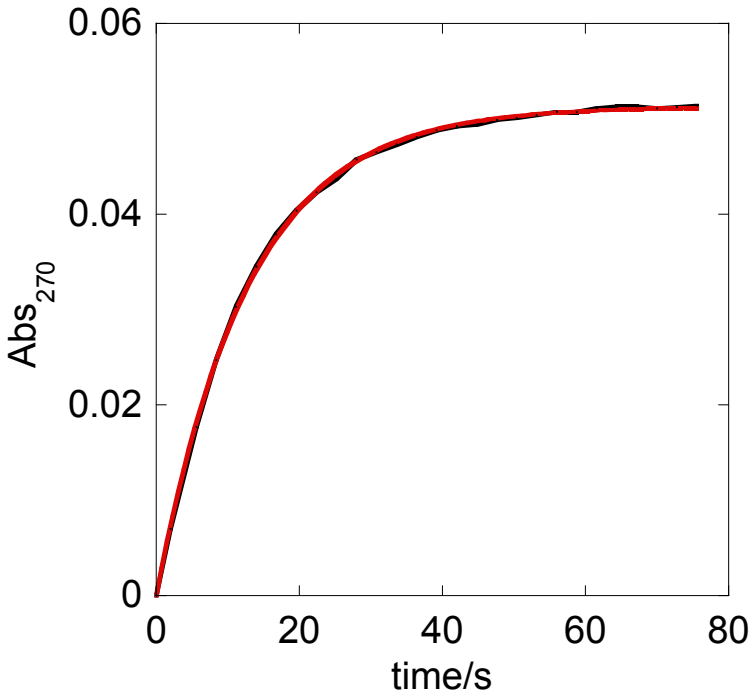

Figure S8. Kinetic (conventional spectrophotometer) trace for a reaction between 0.020 mM Fe(II) and 0.78 mM H_2O_2 at 0.98 M DMSO, pH 6.2 (0.6 mM MES)

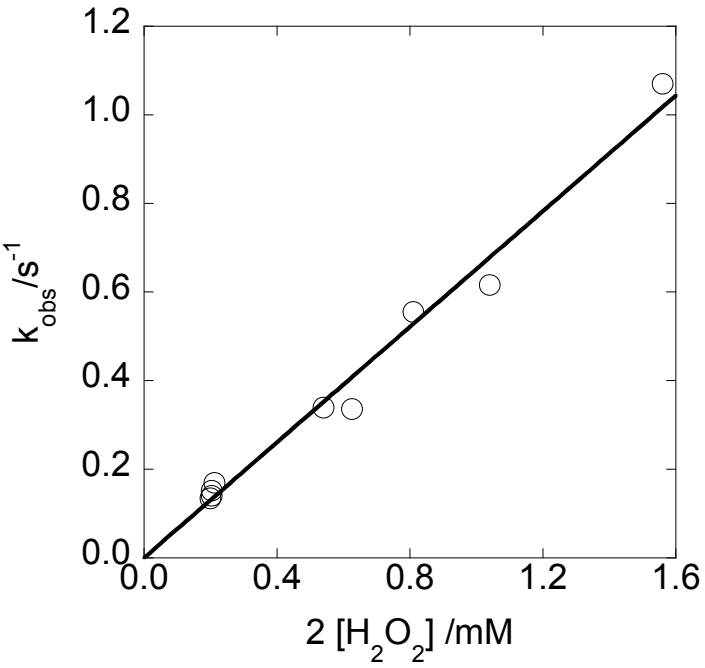

Figure S9. Plot of k_{obs} vs $2[H_2O_2]$ for the Fe(II)/ H_2O_2 reaction at pH 6.1 in MES buffer. Conditions: $[Fe(ClO_4)_2]_0$ = 0.005 – 0.035 mM, [MES] = 0.25 – 0.55 mM, 25 °C. The pH decreased during the reaction by 0.2 units, see text.

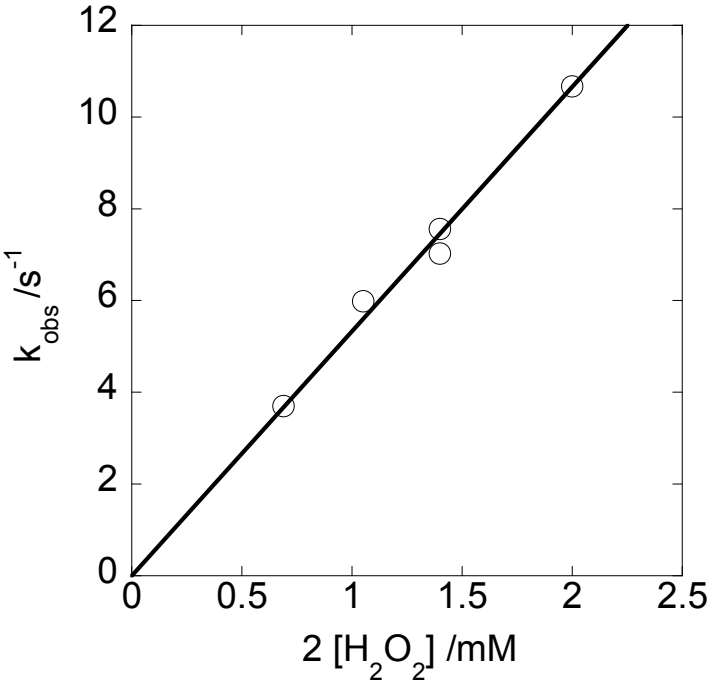

Figure S10. Plot of k_{obs} vs $[H_2O_2]$ for the Fe(II)/ H_2O_2 reaction at pH 7 in a MOPS buffer. Conditions: $[Fe(ClO_4)_2]_0$ = 0.008 – 0.015 mM, [MOPS] = 0.5 - 0.6 mM, 25 °C. pH decreased during the reaction by 0.2 units, see text.

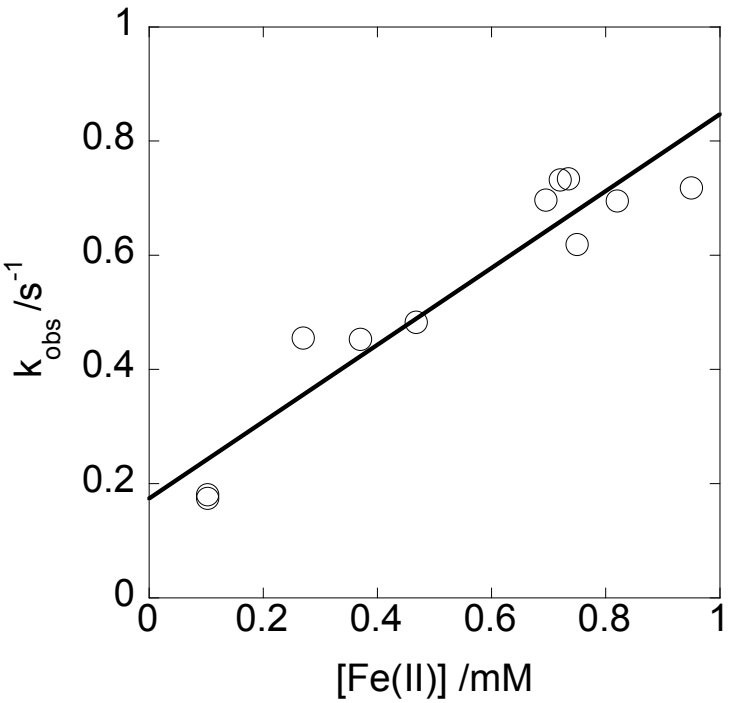

Figure S11. Plot of k_{obs} vs [Fe(II)] for the Fe(II)/ H_2O_2 reaction at pH 6.1 in a MES buffer. Conditions: $[H_2O_2]_0$ = 0.005 - 0.02 mM, [MES] = 0.5-0.6 mM, 25 °C. pH decreased during the reaction by 0.2 units, see text.

Comment on Figure S11. The scatter of the points in Figure S11 is larger than in experiments with excess H_2O_2 (Figs S9 - S10). The plot also exhibits an apparent intercept, but overall the data are in agreement with those obtained with excess H_2O_2 in that the slope of the line in Figure S11 (k_{Fe} = 670 ± 70) $M^{-1}s^{-1}$) is comparable to that obtained by plotting k_{obs} against 2$[H_2O_2]$ in Figure S10 (k_{Fe} = 652 ± 19 $M^{-1}s^{-1}$) for experiments using excess H_2O_2. These results are as expected for the 2:1 [Fe(II)]/$[H_2O_2]$ stoichiometry that was also calculated directly from the observed absorbance changes in these experiments. All of the experiments on catalytic oxidation of sulfoxides required (by definition) excess H_2O_2, conditions that exhibited clean kinetic behavior as shown in Figures S9 and S10.

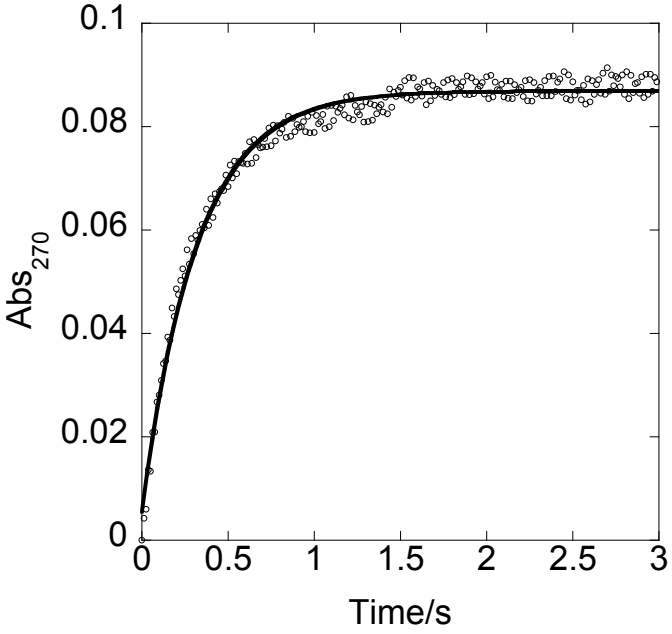

Figure S12. A representative kinetic trace in phosphate buffer. Conditions: 0.031 mM Fe(II), 1.0 mM H_2O_2, pH 6.1 (0.6 mM phosphate buffer)

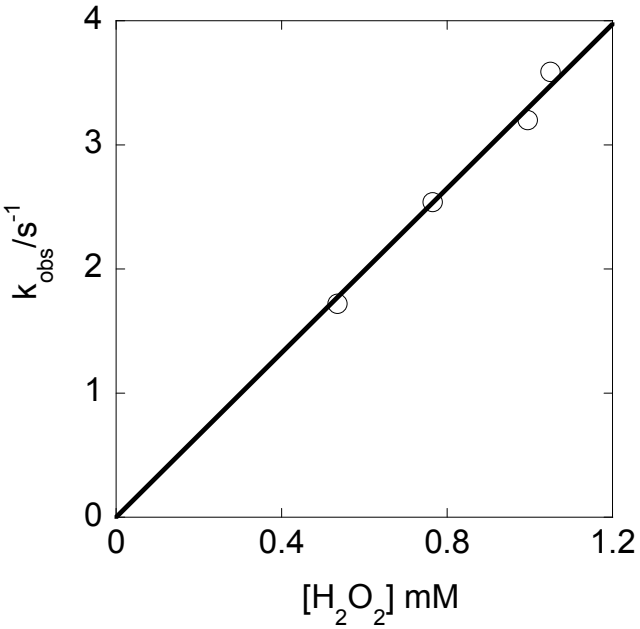

Figure S13. Plot of pseudo-first-order rate constants for the reaction of $Fe(ClO_4)_2$ with H_2O_2 against the concentration of H_2O_2 in phosphate buffer. Conditions: $[Fe(ClO_4)_2]$ = 0.018 – 0.030 mM, [phosphate] = 0.60 mM, pH = 6.1-6.2.

Comment on noninterference of buffers.

Despite the large rate constant reported for the reaction of $HO^{\bullet}$ with tertiary amines k = (2-3) × 10^9 $M^{-1}s^{-1}$,[S5] this reaction cannot be important under our conditions even if $HO^{\bullet}$ radicals were involved. This is so because the rate constant for the $(CH_3)_2SO/HO^{\bullet}$ reaction is even larger, k_{DMSO} = 7 × 10^9 $M^{-1}s^{-1}$, and the concentration of $(CH_3)_2SO$ was also always much higher (and never less than four times higher) than the buffer concentration, so that inequality $k_{DMSO}[(CH_3)_2SO] >> k_{buffer}[buffer]$ held true in every experiment.

In acidic solutions, where the Fenton reaction generates $HO^{\bullet}$, we observed no change in the products of $Fe(H_2O)_6^{2+}/H_2O_2/(CH_3)_2SO$ reaction in the presence of added MES, as shown in Figure S14a [In addition to sulfinic acid and ethane, the reaction in acidic solutions also produces small amounts of the sulfone in a minor parallel path that does not involve Fe(IV)].[S6] The lack of reactivity at nitrogen in acidic solutions is caused by protonation, but the rate constants for hydrogen atom abstraction from C-H bonds are not expected to change significantly between pH 1 and pH 6. The addition of H_2O_2 to MES in the absence of $Fe(ClO_4)_2$ also had no effect on the NMR spectrum of MES (Figure S14b), as expected on the basis of literature data.[S7]

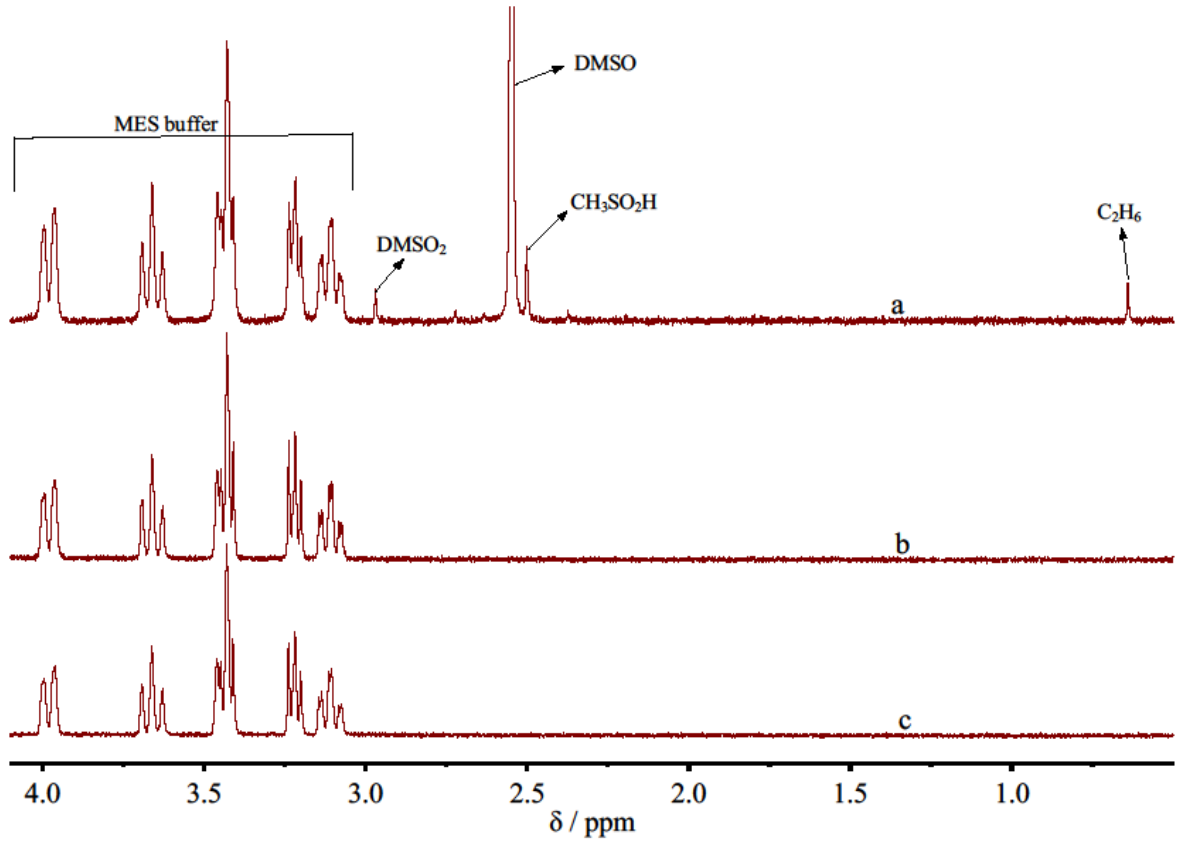

Figure S14. (a) ^{1}H NMR spectrum of the reaction mixture after the completion of the reaction between $Fe(ClO_4)_2$ (1.0 mM), H_2O_2 (1.0 mM), and $(CH_3)_2SO$ (5 mM) at pD 1 in the presence of 5 mM MES. The reaction generated CH_3SO_2H and C_2H_6 in amounts comparable to those obtained in the absence of MES. b) Mixture of MES (5 mM) and H_2O_2 (1 mM), pD 1. c) MES (5 mM), pD 1.

We also ruled out any reaction between the buffers and Fe(IV), the actual intermediate in the Fenton reaction at pH ≥6, by observing that the change in buffer concentration (MES, 10 mM - 24 mM, pD 6.7) under standard conditions (1.2 mM Fe(II), 1.1 mM H_2O_2, 36 mM $(CH_3)_2SO$) had no effect on the yield of sulfone.

References

(S1) Pestovsky, O.; Bakac , A. *J. Am. Chem. Soc.* **2004**, *126*, 13757-13764.
(S2) Kandegedara, A.; Rorabacher, D. B. *Anal Chem* **1999**, *71*, 3140-3144.
(S3) Pestovsky, O.; Bakac, A. *Inorg. Chem.* **2006**, *45*, 814-820.

(S4) Richens, D. T. *The Chemistry of Aqua Ions*; Wiley: Chichester, 1997.
(S5) Halliwell, B.; Gutteridge, J. M. C.; Aruoma, O. I. *Anal. Biochem.* **1987**, *165*, 215-219.
(S6) Pestovsky, O.; Stoian, S.; Bominaar, E. L.; Shan, X.; Münck, E.; Que, L. J.; Bakac, A. *Angew. Chem., Int. Ed.* **2005**, *44*, 6871-6874.
(S7) Zhao, G.; Chasteen, N. D. *Anal. Biochem.* **2006**, *349*, 262-267.